PERGAMON

International Journal of Heat and Mass Transfer 44 (2001) 1767–1776

International Journal of HEAT and MASS TRANSFER

www.elsevier.com/locate/ijhmt

Determination of airside heat transfer coefficient on wire-on-tube type heat exchanger

Tae-Hee Lee [a], Jeom-Yul Yun [a,*], Jang-Seok Lee [a], Jong-Jin Park [a], Kwan-Soo Lee [b]

[a] *Home Appliance Research Lab., LG Electronics Co., 327-23 Gasan-Dong, Keumchun-Gu, Seoul 153-023, South Korea*
[b] *School of Mechanical Engineering, Hanyang University, Seoul 133-791, South Korea*

Received 28 October 1999; received in revised form 1 June 2000

Abstract

Experiments were conducted to obtain the correlation on the airside heat transfer coefficient of wire-on-tube type heat exchangers using single layer samples. Correction factors to the Zhukauskas correlation were determined from the experimental results. Numerical analysis and experiments were performed to validate the applicability of these correction factors using three wire-on-tube type condensers. The results show that the average discrepancy between the performance experiments and present numerical results using the correction factors obtained from this study and Zhukauskas correlation shows 3.7%, while it was 24.7% when the existing correlation was used. © 2001 Elsevier Science Ltd. All rights reserved.

1. Introduction

Wire-on-tube type heat exchanges which has probably been the most widely used condenser in small refrigerant system for many years consists of tube bundles in which a heat transfer medium such as refrigerant is forced to flow, while a second heat transfer fluid like air is directed across the tubes. Since the airside thermal resistance of this heat exchanger is much higher than that of refrigerant side, enhanced surfaces such as wires straightly welded on the series of tubes are employed to effectively reduce the resistance as in the other finned tube heat exchangers, as shown in Fig. 1. Although these are widely used in home refrigerator on accounts of low cost and easy making, the general design data and correlation for the airside heat transfer coefficient are not easily available. This seems to be so because more studies have focused on the research area such as cycle matching and frosting.

The airside heat transfer coefficient of this heat exchanger, in general, can be calculated using the following two methods: (i) The heat transfer coefficient of tubes and wires can be obtained, respectively, by multiplying Zhukauskas correlation [1] by correction factor; (ii) Their results can be formulated directly by performing the heat transfer experiment on wire-on-tube heat exchanger. There have been some related investigations. Jaster [2] used the former method, where he defined 1.0 as correction factor for parts (wire or tube) cross to the air flow and 0.5 as correction factor for parts parallel to the air flow based on Zhukauskas correlation. Hoke et al. [3] has recently presented an empirical correlation on the airside heat transfer coefficient using more than 1600 data from the eight wire-on-tube type heat exchanger. However, this correlation is not easily available despite the fact that the correlation is obtained using relatively large number of data, since the range of error for their data is up to $\pm 20\%$ and their absolute values are much smaller than the exact values based on numerical results of this study.

There have not been enough studies on the performance prediction and design of wire-on-tube type heat exchanger for condenser in refrigerator, and also their data do not correlate well. Hence, an establishment

* Corresponding author. Tel.: +82-2-688-3118; fax: +82-2-856-0313.
E-mail address: jyyun@channeli.net (J.-Y. Yun).

PII: S0017-9310(00)00201-5

Nomenclature

A	heat transfer surface area (m^2)
C	correlation constant
c_p	specific heat at constant pressure ($kJ\,kg^{-1}\,K^{-1}$)
D	diameter (m)
F_c	correction factor in cross flow, Eq. (13)
F_p	correction factor in cross flow, Eq. (16)
G	volumetric flow rate ($m^3\,min^{-1}$)
h	heat transfer coefficient ($W\,m^{-2}\,K^{-1}$)
K	thermal conductance ($W\,K^{-1}$)
k	thermal conductivity ($W\,m^{-1}\,K^{-1}$)
L	length (m)
$\dot{m}$	mass flow rate ($kg\,h^{-1}$)
N	the number of article
NTU	number of transfer unit, $((\eta_s A_T h)/(\dot{m}c_p)_a)$
P	pressure (bar)
Pr	Prandtl number, $Pr = \nu/\alpha$
q	heat transfer rate (W)
Re	Reynolds number, $Re = (\rho VD)/(\mu)$
S	spacing (m)
T	temperature (°C)
U	uncertainty
U_G	gas velocity in case of all refrigerant is assumed with gas ($m\,s^{-1}$)
V	air velocity ($m\,s^{-1}$)
W	width (m)
x	quality

Greek symbols

ε	effectiveness, $(q_{actual})/(q_{max})$
η_s	surface efficiency, Eq. (6)
η_w	fin efficiency of wire
ψ	enhancement factor, Eq. (20)

Subscripts

a	air
AC	all cross
av	average
c	cross flow
cr	critical
cal	calculation
cond	condensation
cor	correlation
exp	experiment
h	heater
H	Hoke's correlation
i	inlet
J	Jaster's correlation
l	liquid
o	outlet
p	parallel flow
r	refrigerant
s	surface
T	sum of tube and wire
t	tube
w	wire
WC	wire cross
wind	wind tunnel
Z	Zhukauskas correlation

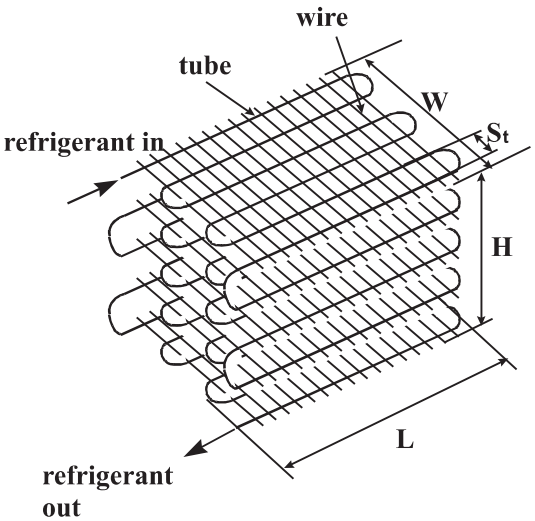

Fig. 1. A shape of wire-on-tube type heat exchanger.

of a reasonable standard for correlation is required. In this study, two empirical correlations obtained from the measurement of airside heat transfer coefficient will be presented. Both the thermal performance test and the numerical analysis on wire-on-tube type heat exchanger are also conducted in order to examine the applicability of the presented correlations, and their results are compared with each other.

2. Measurement of heat transfer coefficient

As far as air flow in wire-on-tube type heat exchanger is concerned, it can be classified into the following three categories based on how each part contacts with air flow:

1. *All cross*. The air passes through both the tubes and the wires.
2. *Wire cross*. The air passes through the wires, whereas it passes along the tubes.
3. *Tube cross*. The air passes through the tubes, whereas it passes along the wires.

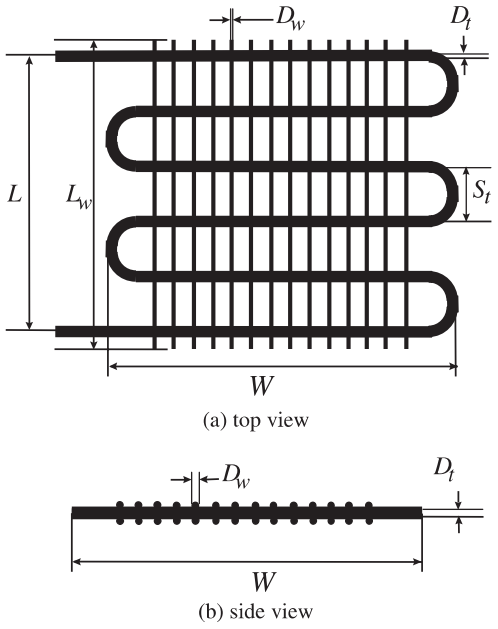

$N_w = 14\times2$, $D_w = 1.55mm$, $D_t = 4.66mm$, $L_w = 154mm$, $L = 140mm$, $W = 220mm$, $S_t = 28mm$

Fig. 2. The single layer of wire-on-tube sample used in this study.

Since its heat transfer characteristics varies with air flow direction due to the structural feature of this heat exchanger, the measurement of the heat transfer coefficient is also required due to the difference in flow structure. The airside heat transfer coefficients are measured from the single layer samples in this study, as shown in Fig. 2. These are applied to both cases of all cross and wire cross. In these works, an electrical heater is used instead of water loop for controlling the heat transfer rate. This has the advantages not only because water loop is not required but also because it can measure the heat transfer rate dissipated to air very accurately.

2.1. Experimental apparatus and procedure

Fig. 3 shows the schematic diagram of the experimental apparatus for measuring the airside heat transfer coefficient using single layer samples of wire-on-tube type heat exchanger. This apparatus is an open type with a small size wind tunnel. It consists of a wind tunnel to measure the air flow rate, a test section with the rectangular duct, a heat supply section to supply the electricity to a line heater inserted into the tube. Four nozzles of 18–60 mm in diameter are installed at a wind tunnel. The measurement error is minimized by opening the nozzle properly for controlling the air flow rate. The air flow rate is calibrated by a pitot tube at the downstream of nozzle, and the deviation between these two data is within 0.3%. The test section is composed of acrylic panel of 10 mm in thickness. 30 mm thick styrofoam is used to minimize the heat loss through the wall in the test section. We have used two test sections of all cross and wire cross. The dimensions of the former are 170 mm in height, 240 mm in width and 600 mm in distance between the entrance and single layer sample, while those of the latter are 15 mm in height, 170 mm in width and 250 mm in distance between the entrance and single layer sample. An example equipped for the case of wire cross is shown in the test section of Fig. 3. The power supply section is composed of a power regulator and a powermeter for controlling and measuring the amount of heat supplied. The powermeter is connected to the data acquisition system.

The inlet air temperature is measured by using the thermopile consisting of 20 junctions and the RTD. The tube surface temperature is obtained by averaging the temperatures measured with 10 type T thermocouples installed at the tube surface. The uncertainty of the

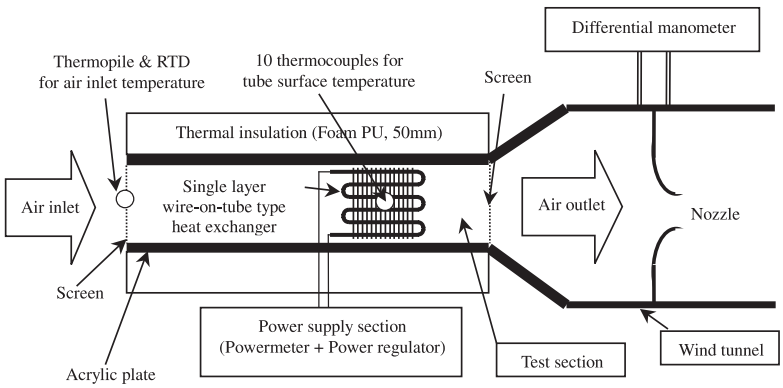

Fig. 3. Schematic diagram of experimental apparatus.

thermopile and the RTD is, respectively, ±0.02°C and ±0.05°C. The tube wall temperature are measured with an uncertainty of ±0.2°C. The air flow rate is determined by using the measured pressure difference with an uncertainty of ±1.5% at the nozzle.

The experiment starts with controlling the electric power after the fan speed reaches a set value. The amount of electric power is measured after the tube wall temperature reaches a steady state at every measuring point. The uncertainties of these experimental results are shown in Appendices A and B.

2.2. Data reduction

The airside thermal contact conductances are obtained as:

$$K_{AC} = (\eta_s A_T h)_{AC} = (\dot{m} c_p)_a \mathrm{NTU}, \tag{1}$$

$$K_{WC} = (\eta_s A_T h)_{WC} = \frac{q_h}{(T_{t,av} - T_{a,av})}, \tag{2}$$

where Eq. (1) represents the case of all cross and Eq. (2) indicates the case of wire cross, respectively. NTU means number of transfer unit and this is calculated with ε–NTU correlation for constant surface temperature.

$$\mathrm{NTU} = -\ln(1-\varepsilon). \tag{3}$$

The effectiveness of a heat exchanger, ε, is obtained as,

$$\varepsilon = \frac{q_h}{(\dot{m} c_p)_a (T_t - T_{a,i})}, \tag{4}$$

where the heat transfer rate, q_h, means the amount of heat supplied into heater. Since the air temperature changes linearly with the air flow direction due to uniform heating for the test heat exchanger, $T_{a,av}$ is calculated by

$$T_{a,av} = T_{a,in} + \frac{q_h}{2\dot{m} c_{p,a}}. \tag{5}$$

As shown in Eqs. (1)–(5), if the amount of heat supplied into heater, the tube surface temperature, the air inlet temperature, and the air flow rate are known from this experiment, the airside thermal conductance obtained by multiplying surface efficiency by heat transfer area and the heat transfer coefficient can be determined. The surface efficiency, η_s, is given by

$$\eta_s = 1 - (1-\eta_w)\frac{A_w}{A_T}, \tag{6}$$

where η_w, A_w and A_T represent the fin efficiency, the heat transfer area of wire and the overall airside heat transfer area, respectively. The fin efficiency, η_w, is given as

$$\eta_w = \frac{\tanh(mL)}{mL}, \tag{7}$$

where

$$m = \sqrt{\frac{4h_w}{k_w D_w}} \quad \text{and} \quad L = \frac{S_t}{2}. \tag{8}$$

Since the fin efficiency of wires is expressed as a function of the heat transfer coefficient, several repeated calculations are required to obtain the fin efficiency and the heat transfer coefficient from the airside thermal conductance. In this study, we neglect the thermal contact resistance between tube and wire, since the wires are welded on tube surface.

2.3. Experimental results

The airside thermal conductance on the wire-on-tube type heat exchanger can be expressed by the sum of tube and fin conductance as follows:

$$K = C_t Re_t^{m_t} Pr^n \frac{k_a}{D_t} A_t + \eta_w C_w Re_t^{m_w} Pr^n \frac{k_a}{D_w} A_w. \tag{9}$$

Since $C_t = C_w$ and $m_t = m_w$ in the case of all cross, K_{AC} is given by

$$K_{AC} = C_c Re_t^{m_c} Pr^n \frac{k_a}{D_t} A_t + \eta_w C_c Re_w^{m_c} Pr^n \frac{k_a}{D_w} A_w. \tag{10}$$

By combining Eq. (10) and Zhukauskas correlation [1], one can find

$$K_{AC} = K_{AC,t} + K_{AC,w} = F_c(h_{Z,t} A_t + \eta_w h_{Z,w} A_w), \tag{11}$$

where $h_{Z,t}$ and $h_{Z,w}$ indicate Zhukauskas correlation on the wire and the tube, respectively. $h_{Z,i}$ is given by [1]

$$h_{Z,i} = C Re_D^m Pr^{0.37} \left(\frac{Pr_f}{Pr_s}\right)^{0.25} \frac{k_a}{D} \quad (i = t \text{ or } w), \tag{12}$$

where constants C and m are varied with the Reynolds number, as shown in Table 1. Thus, the correction factor to Zhukauskas correlation in the case of all cross can be expressed by

$$F_c = \frac{K_{AC}}{h_{Z,t} A_t + \eta_w h_{Z,w} A_w}, \tag{13}$$

where K_{AC} is obtained from the experiment.

Although $C_t \neq C_w$ and $m_t \neq m_w$ in case of wire cross, K_{WC} can be defined by crossing the air to the wire as follows:

Table 1
Values of correlation constants C and m in Eq. (10)

Reynolds number	C	m
1–40	0.75	0.4
40–1000	0.52	0.5
1000–2×10^5	0.26	0.6
2×10^5 – 2×10^6	0.023	0.8

$$K_{WC} = C_p Re_t^{m_p} Pr^n \frac{k_a}{D_t} A_t + \eta_w C_c Re_w^{m_c} Pr^n \frac{k_a}{D_w} A_w. \quad (14)$$

By combining Eq. (14) and Zhukauskas correlation, one obtains

$$K_{WC} = F_p h_{Z,t} A_t + \eta_w F_c h_{z,w} A_w. \quad (15)$$

Thus, the correction factor to Zhukauskas correlation in the case of wire cross is given by

$$F_p = \frac{K_{WC} - \eta_w F_c A_w h_{Z,w}}{h_{Z,t} A_t}, \quad (16)$$

where K_{WC} and F_c are obtained from the experiment and Eq. (13), respectively.

2.3.1. The case of all cross

Fig. 4 shows the airside thermal conductance divided by $Pr^{0.37}$ in the case of all cross, where wires and tubes are all perpendicular to the air flow. The airside thermal conductance (K_{AC}) on the single layer samples obtained from experiment, the tube conductance ($K_{AC,t}$) and the wire conductance ($K_{AC,w}$) are presented together in this figure. As shown in Fig. 4, although the heat rate transferred to wire is slightly different due to the Reynolds number, it indicates that it is equivalent to almost 60% of total heat transfer rate. This is because the heat transfer coefficients are increased due to the fact that outside diameters of wire are far smaller than those of tube, although area ratios of wire and tube are almost equal. It indicates that the ratio of the value calculated from Zhukauskas correlation to the value obtained from the experiment, F_c, has constant value regardless of the Reynolds number, as presented in Fig. 5, and it is derived as follows:

$$F_c = 1.3. \quad (17)$$

The reason for its value above 1.0 is because the heat transfer is far better due to crossing of the air flow on both wires and tubes. This result disagrees with Hoke's result in which Zhukauskas correlation is overestimated in comparison with the actual value.

2.3.2. The case of wire cross

Fig. 6 shows the airside thermal conductance divided by $Pr^{0.37}$ in the case of wire cross, in which the air passes through the wires, whereas it passes along the tubes. The airside thermal conductance on the single layer samples from the experiment, the tube conductance and the wire conductance are presented together in this figure. Although the ratio of the heat rate transferred for the wires is decreased with the Reynolds number, it is equivalent to 77–70% of total heat transfer rate on the average.

Fig. 7 shows the variation of F_p with the Reynolds number. Its value increases slowly with the Reynolds number, and is expressed by

$$F_p = 0.063 Re_{Dt}^{0.37}. \quad (18)$$

It is shown that this correlation predicts all of their data within ±6.8%.

The data obtained by multiplication of these correction factors by Zhukauskas correlation are compared with the experimental result in Fig. 8. As a result, 90% of their data are correlated to within ±2% and all the data are correlated to within ±2.5%.

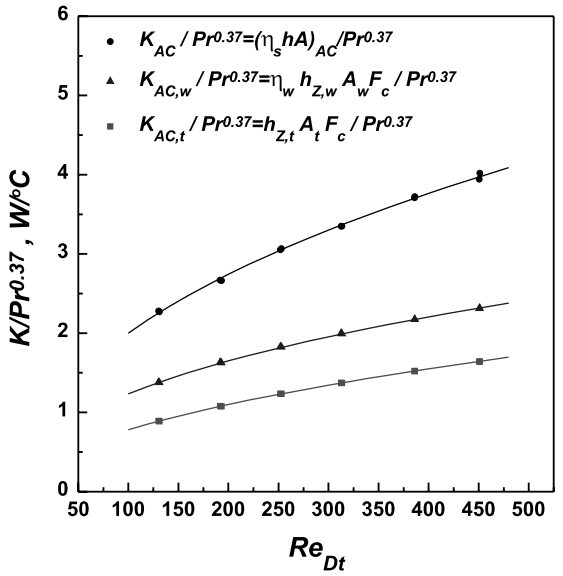

Fig. 4. The variation of heat conductance with Reynolds number based on tube diameter (all cross).

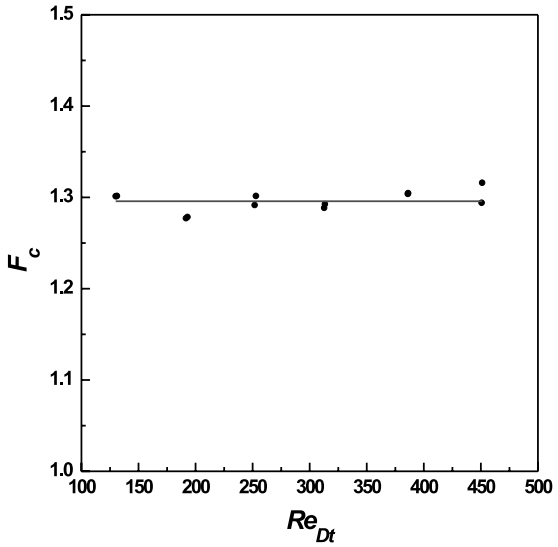

Fig. 5. Correction factor in cross flow (F_c).

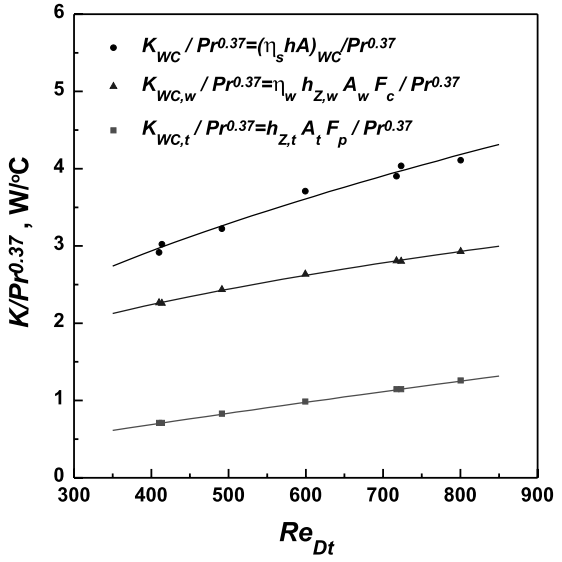

Fig. 6. The variation of heat conductance with Reynolds number based on tube diameter (wire cross).

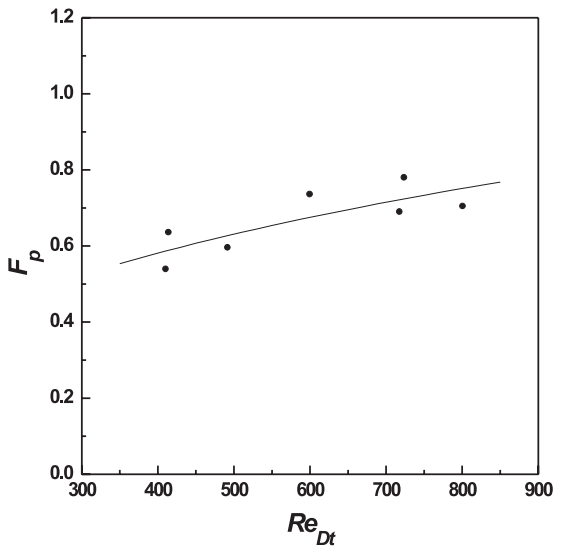

Fig. 7. Correction factor in parallel flow (F_p).

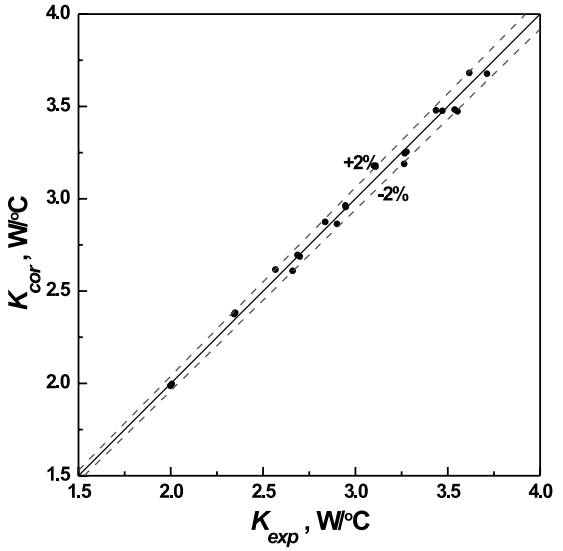

Fig. 8. Comparison of experimental heat conductance and correlation.

3. Investigation on the applicability of correction factor

In this study, the correction factors on the airside heat transfer coefficient are obtained using the ratio of the existing correlation to the airside heat transfer coefficient obtained by this experiment. The applicabilities on these correction factors are investigated by comparing the result of a numerical simulation with a thermal performance test using three wire-on-tube type condensers. The specifications used are presented in Table 2.

3.1. Performance experiment

The experimental apparatus used in this experiment consists of a psychrometric chamber, a refrigerant supply unit and an open type wind tunnel including a test section, as shown in Fig. 9. The refrigerant-side and the airside inlet condition are, respectively, controlled by using the refrigerant supply unit and the psychrometric chamber, and the air flow rate is obtained by controlling the rpm of fan. The refrigerant supply unit consists of compressor, condenser, subcooler, preheater, test section, after heater, and suction unit. The dimensions of

Table 2
Specifications of the three wire-on-tube type condenser used in this study

	A_T (m^2)	A_t (m^2)	D_t (m^2)	L_t* (m^2)	A_w (m^2)	D_w (m^2)	L_w (m^2)
Cond. 1	0.32	0.16	4.76	10.9	0.15	1.53	158
Cond. 2	0.30	0.10	4.76	6.8	0.20	1.53	142
Cond. 3	0.39	0.13	4.76	8.8	0.26	1.53	142

* L_t means total length of tube.

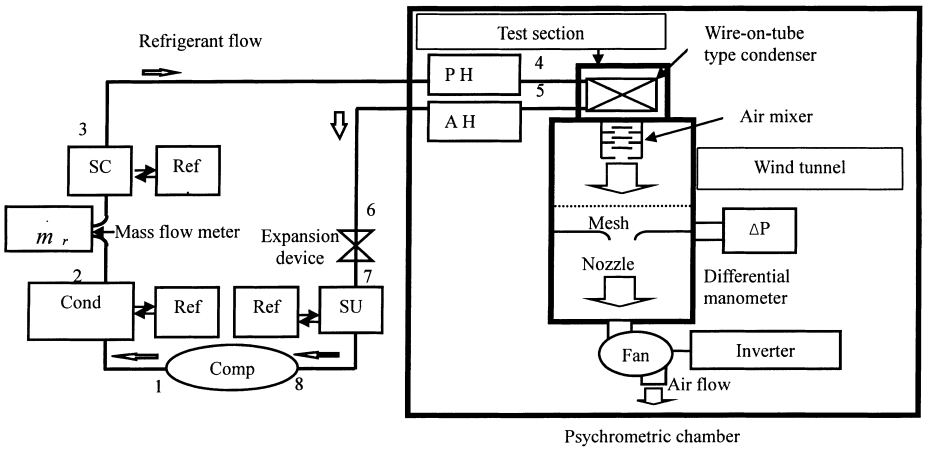

Fig. 9. Schematic diagram of experimental apparatus.

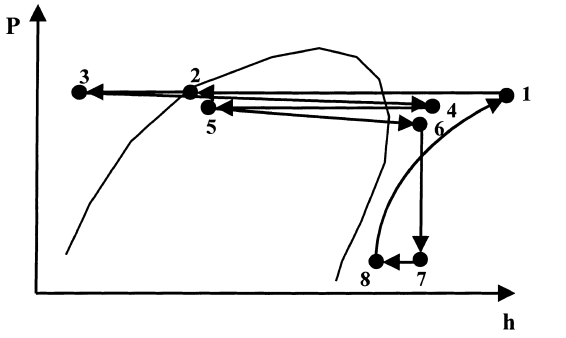

12 : Condenser **56 : After heater**
23 : Sub cooler **67 : Expansion device**
34 : Pre-heater **78 : Suction unit**
45 : Wire-on-tube heat exchanger **81 : Compressor**

Fig. 10. P–H diagram on the thermal performance test.

the test section are 200 mm in height by 200 mm in width. This experiment starts by inputting the condensing pressure, the evaporating pressure, and the inlet temperature of the test heat exchanger. A steady state is always accomplished after about 4 h.

Fig. 10 shows P–H diagram on the thermal performance experiment of the wire-on-tube type heat exchanger. The performance on the test heat exchanger is measured at the point between 4 and 5. The test heat exchanger is installed at the test section of the wind tunnel. The inlet air temperature is measured by using the thermopile consisted of 26 type T thermocouples and the RTD installed at the inlet of test section. The exit air temperature is measured by using the thermopile consisted of 20 type T thermocouples and the RTD installed at the exit of the air mixer in the test section. The uncertainty of the thermopile and the RTD on the inlet and exit temperature is, respectively, ±0.02°C and ±0.05°C. The air flow rates are determined by using the measured pressure difference (0–117 mm H_2O, uncertainty, ±1.5% F.S.) at the nozzle (diameter 35 mm) of the wind tunnel. The inlet temperature condition and the air flow rates are controlled by a psychrometric chamber and a fan with inverter, respectively. 50 mm thick polyurethane foam is used to minimize the heat loss through the wall of the test section and wind tunnel.

The refrigerant-side, airside test conditions and the test results for validating the applicability on the correction factors are presented in Table 3. The heat balance in the wind tunnel and the uncertainty of these experimental results are shown in Appendices A and B.

3.2. Numerical simulation

The section-by-section method [4] is applied for the numerical simulation, which is similar to tube-by-tube method proposed by Domansky [5]. The tube-by-tube method divides a heat exchanger into several tubes, while this method divides a tube into several sections. Shah's correlation [6] is used to calculate the refrigerant-side heat transfer coefficient as follows:

$$h_r = 0.023 \frac{k_l}{D_i} Re_l^{0.8} Pr_l^{0.4} \psi, \tag{19}$$

$$\psi = \left[(1-x)^{0.8} + \frac{3.8 x^{0.76} (1-x)^{0.04}}{P_r^{0.38}} \right], \tag{20}$$

where Re_l is the Reynolds number, Pr_l means the Prandtl number of liquid refrigerant, P_r indicates P/P_c as reduced pressure. In this case, all the refrigerant flowing into the tube is assumed to be a liquid phase. The application ranges of these equations are presented in Shah's work [6]. The airside heat transfer coefficients

Table 3
Test conditions and results for investigating the availability of correction factors

Number of cond.	Flow direction	Test No.	G_a (m^3 min^{-1})	$T_{a,i}$ (°C)	$\dot{m}_r$ (kg h^{-1})	$T_{r,i}$ (°C)	$T_{r,cond}$ (°C)	q_{exp} (kcal h^{-1})
Cond. 1	All cross	1	1.901	29.4	3.96	63.1	36.8	88.6
Cond. 1	All cross	2	1.553	29.5	3.99	63.4	36.8	76.0
Cond. 1	All cross	3	1.210	29.6	3.97	63.4	36.8	64.4
Cond. 1	All cross	4	0.924	29.6	3.99	63.5	36.7	52.1
Cond. 1	Tube cross	5	1.920	29.4	3.98	64.8	36.7	79.9
Cond. 1	Tube cross	6	1.692	29.5	3.94	64.7	36.8	76.7
Cond. 1	Tube cross	7	1.408	29.7	3.97	64.6	36.8	70.0
Cond. 1	Tube cross	8	0.924	29.7	3.95	64.7	36.8	55.0
Cond. 1	Wire cross	9	1.939	29.7	3.99	63.2	36.8	77.9
Cond. 1	Wire cross	10	1.551	29.4	3.95	63.1	36.7	66.9
Cond. 1	Wire cross	11	1.212	29.8	3.99	63.1	36.8	58.9
Cond. 1	Wire cross	12	0.897	29.7	4.03	63.3	36.8	50.6
Cond. 2	All cross	13	1.920	29.6	3.93	63.9	36.8	87.4
Cond. 2	All cross	14	1.510	29.8	3.96	63.9	36.8	74.7
Cond. 2	All cross	15	1.250	29.6	3.99	64.0	36.7	69.1
Cond. 2	All cross	16	0.790	29.7	3.89	63.9	36.8	52.0
Cond. 3	All cross	17	1.910	29.6	4.04	65.9	36.8	95.9
Cond. 3	All cross	18	1.207	29.7	4.00	65.9	36.8	70.9
Cond. 3	All cross	19	0.907	29.8	4.01	66.1	36.8	61.3

used in the numerical analysis are calculated using both the correction factors from this study and Zhukauskas correlation. The application procedure of correction factors used in this case is shown in Table 4. The air flow rate in each section of heat exchanger can be calculated from multiplying air velocity by the sectional area of the airside flow, where the air flow rate in the highest and lowest sections, plus the air flow rate in the right- and left-side sections among them are obtained from multiplying those in the other section by 2.0, respectively. This is because a great deal of air is also flowing to the outside of edge section in the heat exchanger.

3.3. Comparison of experiment and analysis results

The results on the thermal performance experiment and the numerical analysis are shown in Table 5 and Fig. 11, respectively. The operating conditions used in both the experiment and the analysis are given in Table 3. The refrigerant used in this study is R-134a. Both the experimental data and the analytical data obtained using the correction factors from this study, the correction factors (1 or 0.5) proposed by Jaster [2], and the correlation proposed by Hoke et al. [3], respectively, are all presented in Table 5. The discrepancy between the analysis result using the correction factors from this study and the experiment result shows maximum 10% and average 3.7%, while that of Jaster's factor shows maximum 11.5% and average 8.1%. Especially, Hoke proposed a correlation that the airside heat transfer coefficient of a wire-on-tube type heat exchanger is smaller than that of a cylinder in the cross flow. As a result, it is shown that the majority of their data have indicated the discrepancy of maximum 47.5% and average 24.7%, and all of their data are underestimated compared to our experimental results. It is clear that the performance prediction using the correction factors found from this study is more accurate than that of the other two studies.

Table 4
Application procedure of correction factors for numerical analysis

Flow type	h in tube	h in wire
All cross	$h_{Z,t} \cdot F_c$	$h_{Z,w} \cdot F_c$
Tube cross	$h_{Z,t} \cdot F_c$	$h_{Z,w} \cdot F_p$
Wire cross	$h_{Z,t} \cdot F_p$	$h_{Z,w} \cdot F_c$

4. Conclusions

In this study, the correlations on the airside heat transfer coefficient have been developed with a type of correction factor using the single layer samples of wire-on-tube type heat exchanger. The applicabilities of the improved correlations based on Zhukauskas correlation have been discussed through the numerical analysis. Our conclusions from the present work are as follows:

1. The ratio of Zhukauskas correlation for a single cylinder to the heat transfer coefficient cross to the air flow in the wire-on-tube type heat exchanger is constant and its value is shown to be 1.3.
2. The ratio of Zhukauskas correlation for a single cylinder to the heat transfer coefficient parallel to the air

Table 5
Comparison of experimental and numerical results for heat transfer rate of wire-on-tube type condenser

Test no.	Q_{exp} (kcal h^{-1})	Q_{calc} (kcal h^{-1})	Error (%)	Q_{Jaster} (kcal h^{-1})	Error (%)	Q_{Hoke} (kcal h^{-1})	Error (%)
1	88.6	88.7	0.1	78.4	11.5	73.7	16.8
2	76.0	78.6	3.3	70.1	7.9	65.9	13.3
3	64.4	67.8	5.3	61.2	4.9	57.6	10.5
4	52.1	57.3	10.0	52.5	0.9	49.4	5.2
5	79.9	83.2	4.1	70.4	11.9	49.3	38.3
6	76.7	70.9	7.6	66.7	13.0	46.2	39.7
7	70.0	63.4	9.4	60.6	13.4	42.1	39.9
8	55.0	53.0	3.6	52.1	5.3	35.8	34.9
9	77.9	75.2	3.5	67.4	10.9	40.9	47.5
10	66.9	69.0	3.1	64.3	3.9	37.4	44.2
11	58.9	60.0	1.9	56.7	3.7	33.6	43.0
12	50.6	54.0	6.7	51.6	1.9	30.8	39.3
13	87.4	88.3	1.0	78.6	10.1	74.3	14.9
14	74.7	75.3	0.8	67.8	9.2	64.3	13.9
15	69.1	68.6	0.7	62.1	10.0	59.0	14.6
16	52.0	51.1	1.8	47.5	8.7	45.0	13.5
17	95.9	97.1	1.3	87.1	9.2	82.6	13.8
18	70.9	72.2	1.7	66.0	6.9	62.9	11.3
19	61.3	58.9	3.9	54.9	10.4	52.4	14.5

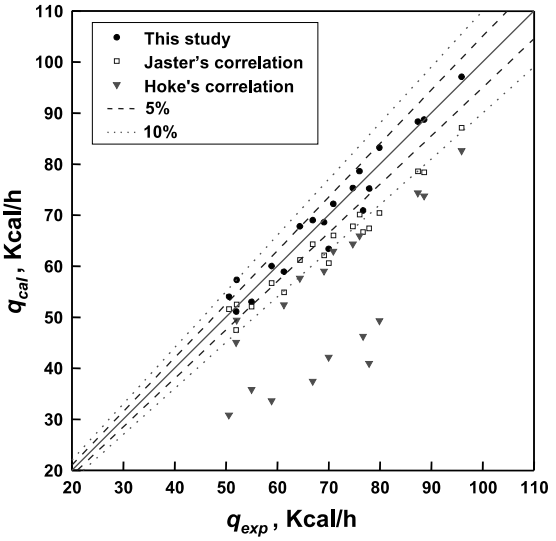

Fig. 11. Comparison of experimental heat transfer rate and calculated heat transfer rate.

flow in the wire-on-tube type heat exchanger is a function of air velocity and it is given by $F_p = 0.063Re_{Dt}^{0.37}$.

3. It is confirmed that the case using the correction factors obtained from this study and Zhukauskas correlation has a more accurate prediction result compared to the existing two cases.

Acknowledgements

One of the authors (Dr. Kwan-Soo Lee) wishes to acknowledge the financial support of Center for Innovative Design Optimization Technology (iDOT), Korea Science and Engineering Foundation (KOSEF).

Appendix A. The uncertainty of thermal conductance

The uncertainty of the airside thermal conductance measurement experiment is expressed as follows:

$$\frac{U_K}{K} = \sqrt{\left(\frac{\partial K}{\partial \Delta T}\frac{U_{\Delta T}}{K}\right)^2 + \left(\frac{\partial K}{\partial C}\frac{U_C}{K}\right)^2 + \left(\frac{\partial K}{\partial q_h}\frac{U_{q_h}}{K}\right)^2}, \tag{A.1}$$

where $\Delta T = T_{t,av} - T_{a,in}$ and the airside thermal conductance are given by

$$K_{AC} = -\bar{C}\ln\left(1 - \frac{q_h}{C\Delta T}\right) \quad \text{and}$$
$$K_{WC} = \frac{q_h}{\Delta T - (q_h/2C)}. \tag{A.2}$$

The resultant uncertainty in measurement is presented in Fig. 12. The uncertainty in the case of wire cross is shown to be below 1%, while the uncertainty in the case of all cross is shown to be 1.7–4.9% because of a larger uncertainty in the temperature difference. Especially when the heat transfer rate of the heater is small, the uncertainty is large.

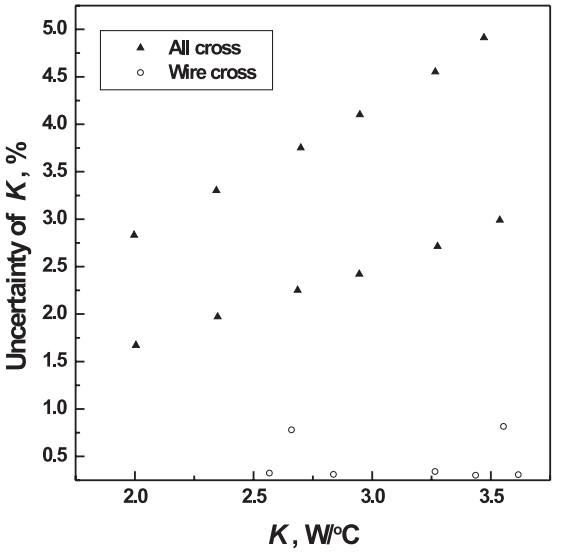

Fig. 12. The uncertainties on the thermal conductance of single layer wire-on-tube sample.

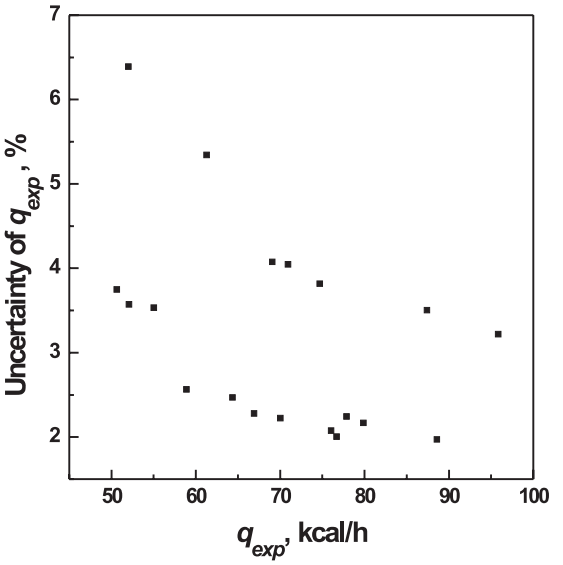

Fig. 13. The uncertainties on the heat transfer rate.

Appendix B. The uncertainty of performance experiment

First of all, the heat balance ratio of a wind tunnel is investigated. The ratio is obtained by comparing the measured airside heat transfer rate with the heating value measured by powermeter, after the electric heater is installed at the test section and the electric power is supplied. An overall error of less than ±3% in the heat balance is permitted in this study.

The uncertainty of the heat transfer rate measured using the wind tunnel which has accuracy of ±3% in the heat balance is calculated as follows:

$$\frac{U_{q_{\exp}}}{q_{\exp}} = \sqrt{\left(\frac{\partial q_{\exp}}{\partial \Delta T}\frac{U_{\Delta T}}{q_{\exp}}\right)^2 + \left(\frac{\partial q_{\exp}}{\partial C}\frac{U_C}{q_{\exp}}\right)^2}, \tag{B.1}$$

where

$$\Delta T = T_{a,o} - T_{a,i} \quad \text{and} \quad q_{\exp} = C\Delta T. \tag{B.2}$$

The resultant uncertainty of the heat transfer rate measured is shown to be 3.5–7.5% as given in Fig. 13. It has high value when the heat transfer rate is small.

References

[1] A. Zhkauskas, J. Ziugzda, Heat transfer of a cylinder in cross flow, Hemisphere, Washington, DC, 1972.
[2] H. Jaster, Analysis of ducted refrigerator evaporators and condensers, GE Report 92CRD163, 1992.
[3] J.L. Hoke, A.M. Clausing, T.D. Swofford, An experimental investigation of convective heat transfer from wire-on-tube heat exchangers, Trans. ASME 119 (1997) 348–356.
[4] T.H. Lee, J.S. Lee, J.J. Park, J.Y. Yun, Effect of tube-to-tube conduction on the performance of an evaporator used in a domestic freezer/refrigerator, Eurotherm Seminar No. 62, 1998, pp. 196–203.
[5] P.A. Domansky, An evaporator simulation model accounting for refrigerant and one dimensional air distribution, NISTIR 89-4133, 1989.
[6] M.M. Shah, Heat transfer during film condensation in tubes and annuli: a review of literature, ASHRAE Trans. 87 (1) (1981) 1068–1105.